RADIOMETRIC ASSESSMENT AND CORRECTION FOR IRS-1C PAN DATA

A. Senthil Kumar, S.K. Limaye, A.S. Kiran Kumar* and K.L. Majumder
Image Processing and Products Division
*Sensor System Division
Space Applications Centre
Ahmedabad 380053 INDIA.

Technical Commission I, Working Group 2

KEY WORDS: Gain settings, CCD Normalization, Signal-to-noise ratio.

ABSTRACT

Radiometric assessment and a normalization procedure using "flat field" data for the IRS-1C PAN detector strips is described in this paper. The flat fields extracted cover almost the entire dynamic range of the detector elements. Our experimental study shows that the odd-even pixel difference and signal-to-noise ratio of the detector array are found to have improved considerably after the normalization.

1. INTRODUCTION

The panchromatic data of IRS-1C spacecraft has created considerable interest in remote sensing community all over the world by virtue of its spatial resolution at 5.8 m [Space Imaging, 1997]. In addition, the PAN payload has also the capacity to tilt upto an angle of ±26 deg. in the direction of pitch for generating stereo image products. An optical layout of the PAN camera is shown in Fig.1. The PAN camera uses basically a reflective optics alongwith three CCD linear array strips for imaging. Each strip has 4096 detector elements (each element of dimension : 7 µm x 7 µm). A special arrangement of an isoceles prism reflector is used to cover all three strips that effectively make a full swath of 70 Km. Each detector has separate interference filters and four light emitting diodes (LEDs) along with a cylindrical lens. Of these four LEDs, two of them are used for optical biassing and the rest two for inflight calibration of the sensor. Four selectable gain settings are also provided for the PAN camera. Other specifications are given in Table 1. [For more details, refer to IRS-1C User Manual, 1995.]

The high data volume of the PAN payload has been taken care by onboard signal processor which facilitates fast reading and processing data from the odd and even pixels in four different channels (two for first 2048 elements and the other two for the rest). The 6 bit PAN data is converted to an 8 bit resolution in the ground data processing while radiometric normalization is carried out. The radiometric normalization coefficients were earlier estimated during the light transfer characteristics (LTC) using six different intensity levels of a calibrated ground truth radiometer (GTR). The LTC data were collected for all four gains and two modes (for normal and redundant detector electronics packages) and for two operating temperatures. Each detector strip was first normalized individually with respect to the minimum radiance at saturation (ie., at 255 count). The strip with the minimum of these three saturation radiances was treated as the reference strip. The inter-strip normalization was carried out by fitting, in the least square sense, the mean values of each strip for the same set of radiance values with that of the reference strip. Finally these normalization coefficients are installed with the help of a radiometric look-up table (RLUT).

It was, however, observed in the post launch data analysis that the odd and even pixel difference was found to be high, especially over low reflecting regions, for the nominal gain G3. This could have probably arisen from the fact that there were not enough GTR values used at the low radiance values while modelling the detector behaviour, and hence the radiometric normalization coefficients have a strong bias toward high radiance values. The result of this was an observable odd-even striping pattern at the Nyquist frequency of the imaging sensor. The result is overall reduction in achievable signal-to-noise ratio (SNR) in the PAN data products.

The odd-even difference can be easily corrected with many scene-based destriping procedures already available in the literature [Horn, 1979; Bizzi, 1996]. These methods are, however, quite tedious and computationally expensive leading to an unacceptable turn around time for the operational 70 Km. PAN data products. We have made an attempt to collect highly homogeneous targets from the PAN data and try to achieve relative radiometric normalization through least square fitting. These homogeneous targets, which we henceforth call "flat fields", are so chosen that the entire dynamic range of the detector array is covered with no single pixel going to saturation level.

2. MATERIAL AND METHOD

Deep ocean, sand and snow data form the natural set of the flat fields desired to cover the sensor dynamic range. Extraction of the flat fields was, however, found to be quite tedious, mainly due to the fact that there exists no defined value of allowable variation (in terms of standard deviation) at the spatial resolution of 5.8 m. We have found that even the so-called dedicated calibration sites, viz., the White sands, the Libyan desert site etc., are all found to have significant standard deviation at this resolution in both the along and the across-track directions of the data. In particular, the sand and snow data were to be extracted using a window search algorithm and patches of most uniform data were combined to form uniform regions. Figure 2 shows the mosaic image of four flat fields. Here we have used two ocean flat fields recorded at different seasons in order to bias the low reflecting areas where the odd-even striping mentioned above is found to be significant.

The normalization using these flat fields is straightforward: The raw flat fields are first radiometrically corrected with the existing RLUT. The mean values of each flat field corresponding to the reference pixel (used in the laboratory LTC exercise) are evaluated and used as the reference values to normalize the other pixels of the sensor array. This gives new slope and offset values of the detector array with respect to radiometrically corrected data. These values are then used to refine the existing slope and offset coefficients of each detector which can correct radiometrically the raw data. Finally, a new radiometric look-up table is generated for direct use with the raw PAN data.

3. RESULTS AND DISCUSSION

Image analysis was carried out over the radiometrically corrected data using the prelaunch and postlaunch RLUT obtained by the method mentioned above. Histogram of odd-even pixel differences and SNR expected at the saturation radiance, obtained by fitting SNRs obtained from different flat fields, quantify the radiometric quality improvement in the data products. Table 2 gives estimated statistical parameters for the flat fields for all the three strips with the prelaunch RLUT. The result of the radiometric normalization described in Sec. 2 are given in Table 3. As can be seen, the SNR has improved considerably, due to the fact that the odd-even difference has reduced. Histograms of odd-even pixel differences are also shown in Fig. 2. The SNR of the centre strip obtained is however slightly under the specification SNR given in Table 1. This can be mostly attributed to the nonuniformity in the flat field data . As noted earlier, realization of ideal flat fields is found to be impractable with any natural homogeneous earth's targets at the spatial resolution of 5.8 m. It is hence required to go for artificial flat field targets in order to achieve better postlaunch radiometric correction.

REFERENCES

Bizzi, S., Arino, O. and Goryl, R., 1996. Operational algorithm to correct the along track and across track striping in the JERS-1 OPS images. Int. J. Remote Sensing. **17** (10), pp. 1963-1968.

Horn, B.K.P. and Woodham, R.J., 1979. Destriping LANDSAT MSS images by Histogram modification. Computer Graphics and Image Processing. **10**, pp. 69-83.

IRS-1C User Manual, 1995. Natioanl Remote Sensing Agency, Hydrabad, India.

Space Imaging EOSAT NOTES, 1997. **12** (1).

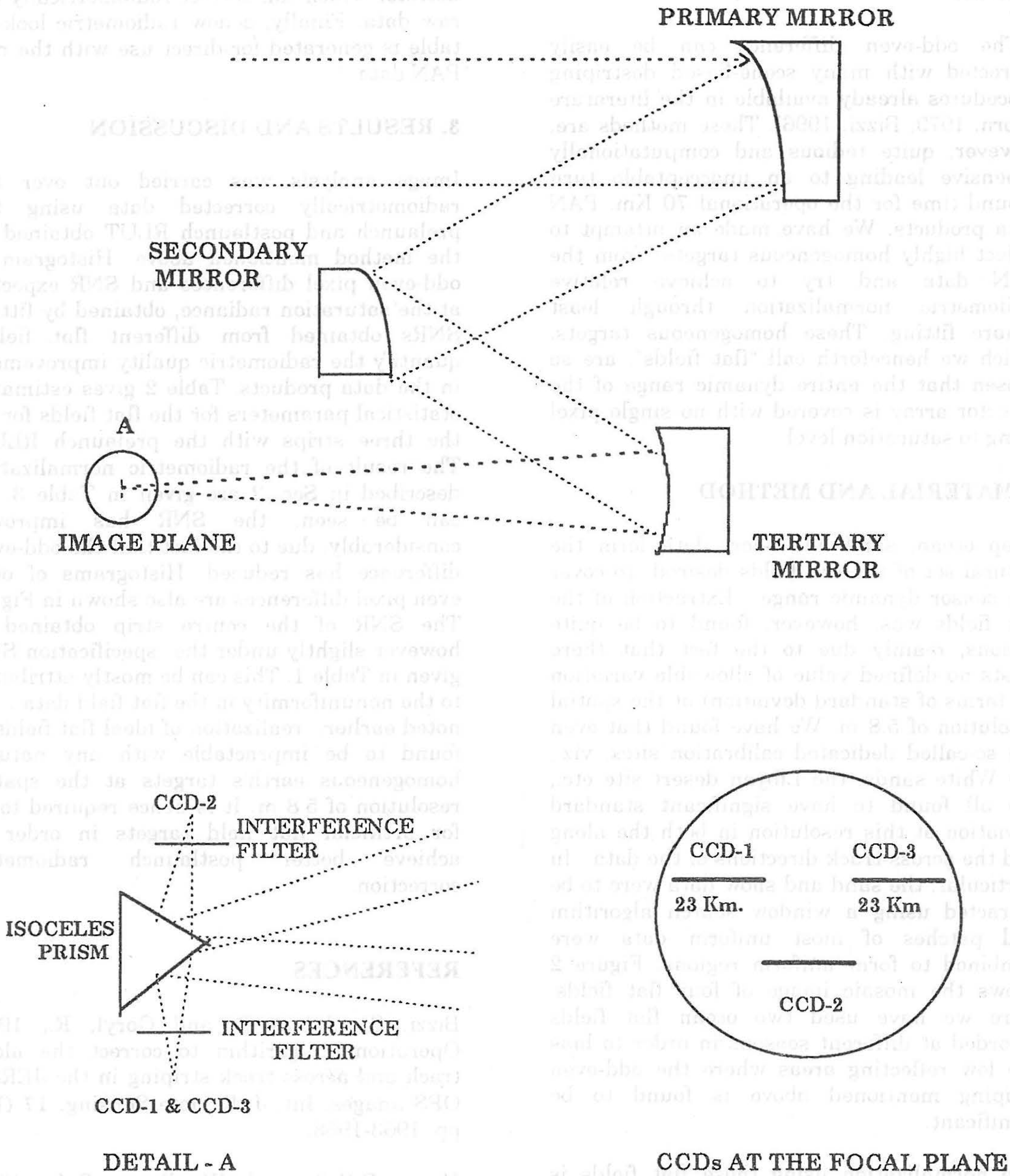

FIG. 1. OPTICAL LAYOUT OF IRS-1C: PAN CAMERA

Table 1. Major specifications and features of IRS-1C PAN Camera.

S. No.	Features	Specifications
1	Instantaneous Field of View	5.8 met.
2	Swath at Nadir View	70 kms.
3	Swath at steering range	± 26 deg.
4	Spectral range	0.50-0.75μm.
5	Square wave response (at Nyquist freq.)	> 0.20
6	Quantization levels (on-board)	6 bits
7	Signal-to-noise ratio (at Sat.Radiance)	> 64
8	Saturation Radiances (mw/(cm*cm-sr-μm)	47.00 (G1) 35.23 (G2) 26.00 (G3) 13.50 (G4)
9	No. of CCD array (strip)	3
10	No.of detector elements in each strip	4096

Table 2b. Radiometric performance of the centre CCD strip with prelaunch RLUT.

Feature extracted	Average Mean	Average Std. Dev.	Range of Mean	Estimated Signal-to-ratio
Waterbody	36.82	2.09	10.60	27.21
Ocean	55.02	3.06	11.23	17.96
Sand	125.56	5.01	16.10	25.05
Snow	163.73	5.08	20.77	32.21

SNR at Saturation Radiance. = 42.50

Table 3b. Radiometric performance of the centre CCD strip with after correction.

Feature extracted	Average Mean	Average Std. Dev.	Range of Mean	Estimated Signal-to-ratio
Waterbody	36.96	1.79	5.10	31.74
Ocean	55.17	2.83	5.35	19.50
Sand	125.82	4.46	10.64	28.19
Snow	164.06	4.14	7.02	39.60

SNR at Saturation Radiance. = 54.05

Figure 2b. Histogram of odd-even pixel difference (a). before and (b). after correction.

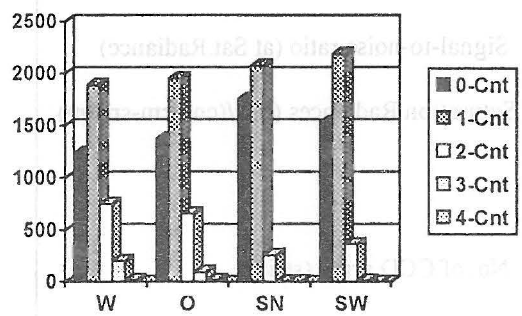

(a)

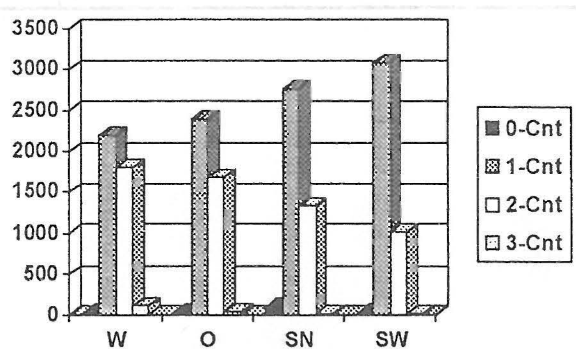

(b)

Table 2a. Radiometric performance of the West CCD strip with prelaunch RLUT.

Feature extracted	Average Mean	Average Std. Dev.	Difference in Odd-Even Chain	Estimated Signal-to-ratio
Waterbody	30.53	1.55	0.422	19.73
Ocean	45.42	3.496	0.60	12.99
Sand	115.15	4.954	0.64	23.24
Snow	153.23	3.924	0.087	39.05
		SNR at Saturation Radiance.	=	62.85

Table 3a. Radiometric performance of the West CCD strip with after correction.

Feature extracted	Average Mean	Average Std. Dev.	Difference in Odd-Even Chain	Estimated Signal-to-ratio
Waterbody	34.05	1.52	0.165	22.37
Ocean	47.06	2.770	0.106	16.99
Sand	107.83	3.135	0.254	34.39
Snow	141.06	2.548	0.173	55.36
		SNR at Saturation Radiance.	=	100.92

Figure 2a. Histogram of odd-even pixel difference (a). before and (b). after correction. Here "W" denotes waterbody; "O" - ocean; "SN"- sand and "SW" - snow features.

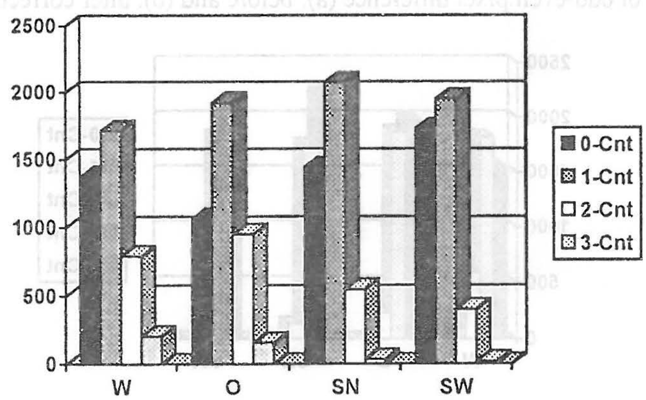

(a).

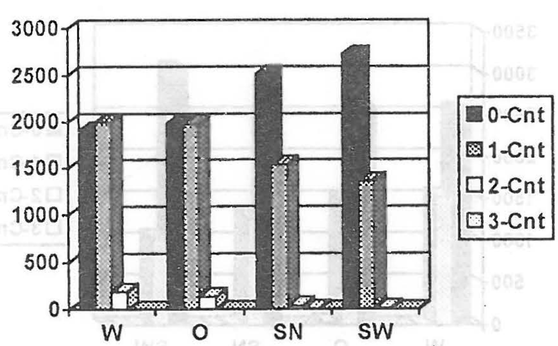

(b)

Table 2c. Radiometric performance of the East-CCD strip with prelaunch RLUT.

Feature extracted	Average Mean	Average Std. Dev.	Range of Mean	Estimated Signal-to-ratio
Waterbody	39.70	1.68	7.10	23.60
Ocean	46.79	3.01	8.63	15.57
Sand	120.26	4.31	14.05	27.90
Snow	161.77	4.74	15.49	34.12

SNR at Saturation Radiance. = 46.92

Table 3c. Radiometric performance of the East-CCD strip with after correction.

Feature extracted	Average Mean	Average Std. Dev.	Range of Mean	Estimated Signal-to-ratio
Waterbody	39.93	1.44	4.91	27.72
Ocean	47.02	2.61	6.22	17.59
Sand	120.32	3.92	10.52	30.72
Snow	161.73	3.68	7.09	43.98

SNR at Saturation Radiance. = 64.98

Figure 2c. Histogram of odd-even pixel difference (a). before and (b). after correction.

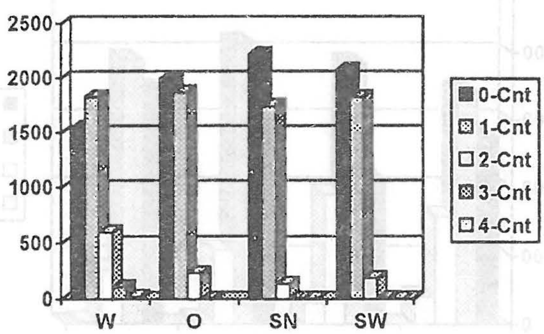

(a)

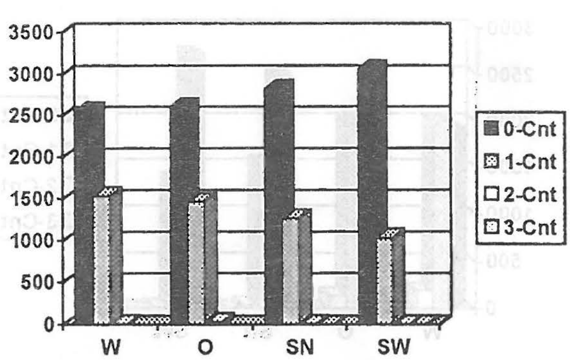

(b)